Hemispheric mPFC Asymmetry in Decision Making under Ambiguity and Risk: an fNIRS Study

Yuhua Li[1], Rui Chen[1], Shuyue Zhang[2], Ofir Turel[3, 4],

Antoine Bechara[2], Tingyong Feng[1, 5], Hong Chen[1, 5] *, Qinghua He[1, 5, 6] *

[1] Faculty of Psychology, Southwest University, Chongqing, China

[2] Department of Psychology, Guangxi Normal University, Guilin, Guangxi, China

[3] Brain and Creativity Institute and Department of Psychology, University of Southern California, Los Angeles, CA, United States

[4] Information Systems and Decision Sciences, California State University, Fullerton, CA, United States

[5] Chongqing Collaborative Innovation Center for Brain Science, Chongqing, China

[6] Southwest University Branch, Collaborative Innovation Center of Assessment toward Basic Education Quality, Chongqing, China

Running Head: MPFC AND DECISION MAKING

*Correspondence should be sent to:

    Dr. Qinghua He
    Faculty of Psychology, Southwest University
    Chongqing, 400715, CHINA
    Tel: +86-13647691390
    Email: heqinghua@gmail.com

OR   Dr. Hong Chen
    Faculty of Psychology, Southwest University
    Chongqing, 400715, CHINA
    Tel: +86- 13883224482
    Email: chenhg@swu.edu.cn

Word Count: Abstract: 167; Introduction: 867; Discussion: 735.

    No. of Tables: 1; No. of Figures: 7.

Declarations of interest: none.

Abstract

The Iowa Gambling Task (IGT) is a commonly used task for testing decision-making under ambiguity (the early stage) and risk (the late stage). However, differences between the temporal dynamic signals underlying these two types of decision-making as well as the hemispheric specificity of decision making during the IGT remain unknown. The present study sought to address this gap by focusing on the medial prefrontal cortex (mPFC), which plays an important role in decision-making across life domains. We used functional near-infrared spectroscopy (fNIRS) with high spatial and temporal resolution and measured oxy-hemoglobin concentration within the mPFC in 25 healthy participants who performed the IGT. Results showed that there are different activations of the right and left hemispheres of the mPFC during the different stages of IGT and types of decisions. This implies that the left and right mPFC can have different patterns of involvement in decision making, at least in IGT decisions, including making good (low risk) and bad (high risk) choices, under ambiguity and under risk conditions.

Keywords: functional near-infrared spectroscopy (fNIRS); decision-making under ambiguity; decision-making under risk; medial prefrontal cortex; Lateralization; Iowa Gambling Task (IGT)

1. Introduction

Decision-making is a high-level cognitive process in humans [1]. It involves weighing alternative outcomes' desirability and probabilities [2-5]. Two broad families of decision-making exist: (1) in deterministic situations, in which several fixed options are available and the individual makes decisions based on subjective value judgments, and (2) in uncertain situations in which the outcomes and/or success probabilities of several options are uncertain. Decision-making under uncertainty is more common, because many events are not fully predictable [6]. Uncertainty can manifest in two forms: ambiguity and risk. While in both forms of uncertainty the outcomes of decision making are not deterministic, they differ in that in decision-making under ambiguity the probability of each outcome is unpredictable while in decision-making under risk there is some explicit knowledge regrading outcome probabilities, but there is still the chance of not obtaining the desired outcome [3,4].

The Iowa Gambling Task (IGT) [7] is a common task used for determining the decision-making ability of individuals. Participants are instructed to choose among four decks of cards: two disadvantageous decks that pay larger rewards but also present larger losses, and two advantageous decks that pay smaller rewards but also present lower losses. Participants are not given these details, and they need to figure out which decks are advantageous during task performance. This learning process takes time; numerous IGT studies have demonstrated that in early stages of IGT probabilities are unknown, and that in later stages people learn to pick more often from advantageous decks [8, 9]. Hence, early stages of IGT can be viewed as decision-making under ambiguity given the unknown payoff probabilities, while late stages are more consistent with decision-making under risk, given the learning that takes place in earlier

stages [10].

The medial prefrontal cortex (mPFC) plays a critical role in decision making, as demonstrated in various IGT studies [11,12]. Patients with mPFC damage showed continuously disadvantageous decisions even after they knew the correct strategy, while normal controls could decide advantageously [13]. However, there is limited knowledge regarding (a) differences in mPFC activation in the two stages of IGT, representing decisions under ambiguity and under risk, and (b) functional inter-hemispheric difference in the mPFC in decisions under risk and ambiguity. We seek to bridge these gaps in this study.

The IGT was primarily developed to test several aspects of the Somatic Marker Hypothesis (SMH), which explained decision-making impairments after frontal lobe damage [14,15]. The SMH proposes that decision-making requires the integration and biological regulation of somatic states that include emotional and affective processes. The marker signal affects decisions unconsciously and/or consciously. It can guide individuals to make advantageous decisions through the encoding of the overall result of a certain behavior. As such, SMH provides a neuroanatomical and cognitive framework for decision-making based on long-term results rather than short-term gains. In addition, it suggests that the decision-making process depends on many important aspects of the neural substrate regulating homeostasis, emotion and feeling [14].

In this framework, the mPFC is considered to be a key structure that triggers somatic states [16]. Early studies of normal subjects established that the pondering of decisions on the IGT was associated with the triggering of skin conductance responses (SCR), which are indicative of somatic states, before making a decision [13,17]. During the early parts of the task, the

triggered SCRs before choosing the advantageous or disadvantageous decks were almost equal. However, as the task progressed, and more knowledge was acquired about success probabilities of different decks, the SCRs before making disadvantageous choices grew larger, while those before the advantageous choices grew smaller [13,17]. Patients with bilateral mPFC lesion never triggered these anticipatory SCRs, and never learned to choose advantageously [13,17]. These results implied that the mPFC plays a key role in triggering these somatic states, which in turn play an important role in guiding decisions. However, direct evidence about the different levels of activity of the mPFC during the different phases of the IGT (early/ uncertainty vs. late/ risk) and in advantageous vs. disadvantageous decisions was not obtained.

The present study addresses this gap by using the IGT task and functional near-infrared spectroscopy (fNIRS) to analyze the time line of mPFC activity during IGT performance. fNIRS captures the distribution and changes of blood volume and blood oxygenation in the cerebral cortex [18]. It has excellent temporal and spatial resolutions [19]. This allows us to observe the temporal dynamic signals of brain activity during the IGT task. fNIRS was used in a similar manner to detect differences in temporal dynamic signals of the dorsolateral prefrontal cortex associated with good and bad IGT decisions [20].

Although the initial SMH description suggested that the right hemisphere is more involved in somatic marker activity [14], there is limited empirical support for this assertion. In light of more recent functional neuroimaging studies suggesting that mPFC activity switches hemispheres as decision-making conditions change from ambiguity to risk [21-23], we hypothesized that the right mPFC would be more active in triggering the "negative" somatic marker associated with disadvantageous decisions. This negative somatic marker is in

line studies showing a high anticipatory SCR before disadvantageous decisions [13,17]. We tested this hypothesis with fNIRS applied to 25 healthy young adults (20 to 25 years old) who performed the IGT.

2. Materials and Methods

2.1. Participants

The study was approved by the Southwest University Institutional Review Board and written informed consent was obtained from all participants before the experiment. Thirty college students (25 females) were recruited via a class announcement at Southwest University. Inclusion criteria were: (1) right-handedness, (2) normal or corrected-to-normal vision, and (3) no history of neurological or psychiatric diseases. Five of them (4 females) were excluded because they continuously chose the same card. Hence the sample was reduced to 25 participants (4 males and 21 females).

2.2. The Iowa Gambling Task

We used a computerized version of the original IGT task, run in Matlab (The MathWorks, Inc., MA, USA) with Psychtoolbox (http://psychtoolbox.org/) [7]. This task and its paradigm have been validated in both behavioral and fMRI studies of normal subjects and patients with brain lesions [5,24,25]. Participants were asked to choose one card at a time from four decks (labeled A, B, C, and D, respectively). They were given a total of $2000 borrowed money from the experimenter at the beginning, so they can play the IGT game. Each participant was asked to make a total of 100 card choices. Each card selection could bring an immediate reward (the immediate reward was higher in decks A and B than in decks C and D), or a loss (in decks A and C there were smaller but more frequent unpredictable punishments, while in decks B and

D punishments were greater but less frequent), thus creating a decision conflict in each choice (see Fig.1a, b and c).

Although the total gains were on average higher in decks A and B than in C and D, the total losses were also higher in decks A and B relative to decks C and D. As such, decks A and B were disadvantageous in the long run (hence called "bad decks"), whereas decks C and D were advantageous in the long term (hence called "good decks"). Specifically, when choosing bad decks continuously in 10 rounds, participants would win $1000 but lose $1250 (resulting a net loss of $250). In contrast, when choosing good decks continuously in 10 rounds, participants would win $500 but lose $250 (resulting in a net gain of $250). The gain or loss stemming from each card was pre-specified following previous studies [7,26]. Participants were instructed to gain as much as possible while avoiding losses. Although each participant received fixed compensation (￥45), they were encouraged and intrinsically motivated to gain as much as possible in the IGT task.

The IGT process is typically divided into two phases. The first represents ambiguity (initial stage); it eventually translates in healthy participants into insights regarding advantageous decks (late stage). The first 40 trials are considered as the early phase (largely consistent with decision-making under ambiguity), and the last 60 trials reflect the late phase (largely consistent with decision-making under risk) [5,6]. We employed this division to stages here (see supplemental material). Nevertheless, to avoid this crude division, we report in the manuscript the division into stages based on the actual pattern of performance on IGT trials. This pattern implied that given the low average performance in blocks 1 and 2 and the much more frequent selection from advantageous decks in blocks 4 and 5, these groups of block can reasonably

represent decision making under ambiguity and risk, correspondingly.

2.3. Multi-channel fNIRS instrumentation and data acquisition

The changes in the oxyhemoglobin (HbO), deoxy-hemoglobin (HbR) and total-hemoglobin (tHb) concentrations were recorded in each channel based on the modified Beer-Lambert law [27] using a multi-channel fNIRS brain imager (FOIRE-3000/16, Shimadzu Corporation, Japan), which affords 16 source-detector sets. During imaging, subjects were asked to sit in a comfortable chair in front of a laptop computer. A fiber-optic probe set with 32 optodes (16 transmitters and 16 receiver optodes, 3cm apart, forming 52 channels) was placed across participants' foreheads to cover the whole medial part of the prefrontal cortex (Fig.2a). Each transmitter fiber delivered three wavelengths of light at 780nm, 805nm and 830nm by light-emitting diodes. The detected fNIRS signals were continuously acquired for the entire task procedure in the frequency of 4 Hz over medial prefrontal cortical areas. The fiber-optic probe set was placed low over the forehead so that the bottom was touching the tops of participants' eyebrows. This ensured adequate coverage of the forehead and resulted in a roughly uniform vertical position among all participants. Before taking the actual recordings, all optodes were checked for adequate contact on participants' scalps. We performed an automatic adjustment of the negative high pressure of photomultiplier and confirmed that the pressure falls within a range of 450 - 650V. Participants completed 100 trials of the IGT, which took an average time of 9 min. There were extra 20 seconds at the beginning and end of the task to warm up the machine and account for the hemodynamic delay of brain response.

We utilized the 3-dimensional (3D) Patriot Digitizer (Polhemus, USA) to locate the neuro-anatomical position of the channels. First, using the recording pen, the locations of Nz (nasion),

Iz (inion), AL (left preauricular point), AR (right preauricular point), Cz (central zero) on the headgear, which were considered as five reference points, were marked. Then, the coordinates of all optodes (including transmit and receive optodes) and channels were recorded. Using NIRS_SPM, a MATLAB-based software package (http://www.nitrc.org/projects/nirs_spm/), we were able to obtain the representation of spatial location of fNIRS channels on a human brain template. The channel-wise individual location data were registered to the standard Montreal Neurological Institute (MNI) space with standalone registration. For all subjects, we calculated average coordinate point of each channel. We then drew a spherical region around the coordinate point with a radius of 15mm (half spatial resolution) to validate the location of each channel.

Fig.2b shows the probe geometry overlaid on the frontal cortices of anatomical images of a human brain. The areas covered by the fNIRS probes were mainly over Brodmann areas (BA) 10, 9, and 46, which cover the mPFC. The left medial prefrontal cortex was covered by channels 28, 35, 36, 42, and 43, and the right medial prefrontal cortex was covered by channels 25, 32, 33, 40, and 41 (Fig.2b, Fig.2c and Table.1). This focused selection allowed us to perform analyses on the regions of interest and reduce the number of comparisons.

2.4. Statistical analysis

2.4.1. Behavioral data

The task was divided into five blocks with 20 trials each, named IGT1-5, respectively. Following common IGT practices [5,6,28], the IGT score of each participant was calculated for each block by subtracting the total number of bad deck selections from the total number of good deck selections [i.e., $(C + D - A - B)$]. Then we calculated the average score of each block for

all participants, and we analyzed the IGT scores in the five blocks by repeated measures analysis of variance (rmANOVA).

2.4.2. fNIRS data

This study focused only on changes in HbO concentration, which is the most sensitive indicator of change in regional cerebral blood flow in fNIRS studies [29,30]. Raw HbO concentration data were entered into a finite impulse response (FIR) function-based General Linear Model (GLM) to represent the hemodynamic response for each channel [31,32].

The FIR model was set to start two seconds before the stimulus onset and continue for another 14 seconds. There was a total of 64 parameters for each event with a 4 Hz sampling rate. The duration of this FIR model (16 seconds) was consistent with the length of hemodynamic response triggered by stimuli [33]. Because we are interested in the decision making process, the onset time for each event was defined as the time a new card choice task was introduced. Four conditions were included in the FIR model: early good decisions, early bad decisions, late good decisions, and late bad decisions.

Good decisions were defined as choosing from decks C and D while bad decisions were defined as choosing from decks A and B. The maximum value of the resulting Hemodynamic Response Function (HRF) served as the index of brain activity for each channel.

For the activation value of each condition in each channel of the bilateral ROIs, one sample t-test was first performed to examine whether this region is activated or not. Then, a $2 \times 2 \times 2$ three-way rmANOVA with Selected Deck Type (good vs. bad), Task Stage (early vs. late) and Brain Hemisphere (left vs. right) as within-subject factors was performed for each channel. To clarify the role of brain hemispheres, we also calculated an asymmetry index, defined as the

activity differences of the left and right mPFC (i.e., left – right) [34]. For this asymmetry index, a 2 × 2 two-way ANOVA was performed, with Selected Deck Type (good vs. bad), Task Stage (early vs. late) as within-subject factors. In addition, a 2 × 2 rmANOVA was performed with Selected Deck Type (good vs. bad) and Task Stage (early vs. late) as factors predicting left and right mPFC activity, separately. Lastly, we calculated the Pearson correlation between brain activation and IGT scores in each block. For all analyses, family-wise errors were accounted for by using False Discovery Rate (FDR) correction with alpha value of 0.05.

3. Results

3.1. Behavioral data

The five 20-trial blocks of the IGT were analyzed, following common procedures [7], See Fig.1D. rmANOVA with the IGT scores of five different blocks as within-subject factor suggested that there was a significant learning over time effect. As participants progressed through IGT blocks they learned to choose advantageously ($F_{(4,96)} = 10.49$, $p < 0.001$, $\eta^2 = 0.304$). A post hoc test showed that there were higher IGT scores in blocks 4 and 5 compared to blocks 1, 2 and 3 [least significant difference test (LSD), $p < 0.05$]. In addition, block2 showed a higher IGT score, compared to block1 (post hoc: $p < 0.05$). The IGT score in block 3 was slightly but not significantly higher than this of block1 (post hoc: $p = 0.057$).

Based on these results, we regarded blocks 1 and 2 (the first 40 trials) as decision making under ambiguity in which probabilities are supposedly not yet well-learned, and regarded blocks 4 and 5 (the last 40 trials) as decision making under risk. The reasonableness of this division is also illustrated in Fig. 3, which portrays the performance on IGT (with 95% Confidence Intervals) for all subjects. It too demonstrates that blocks 4 and 5 participants'

performance was significantly better than their performance in the first two blocks. This is indicative of a learning effect that matured, on average, after the first three blocks, during block 3. Furthermore, the paired sample t-test conducted for early stage (the first 40 trials, i.e., block1 + block2) and late stage (the last 40 trials, i.e., block4 + block5) showed a significant difference in IGT scores (M_{early}= 0.04, M_{late}= 6.48, $t_{(24)}$= -5.49, p < 0.001, *Cohen's d = -2.241*). Altogether, these analyses suggested that participants learned to choose more advantageously in the late stage relative to the early stage. Given that the subjects were cognitively healthy; it was reasonable to attribute improvements in IGT scores to learning mechanisms.

3.2. fNIRS data

3.2.1. *Both left and right mPFC regions were activated during decision making*

We commenced analysis with a channel-wise activity check. Results suggested that every channel within the left and right mPFC was significantly active (showed a significant hemodynamic response to the stimulus) during the four different conditions of the task (Fig.4).

3.2.2. *The left and right mPFC have different patterns of involvement in decision making under ambiguity and under risk conditions*

To reduce the amount of multiple comparisons, we averaged the hemodynamic signals from each channel within each ROI. Fig.5A plots the average time course of left and right mPFC activation over all participants in the different conditions. The progression pattern highlights the centrality of the mPFC in decision making. The differences between the activity progression lines, each representing a different decision stage (early/late) and choice type (good/bad), hints at possible differential involvement of the mPFC in different decision stages and choices.

We next tested whether there are left and right mPFC activation differences in the different conditions of the IGT. To do so we estimated a 2 (Selected Deck Types: good vs. bad) × 2 (Task Stages: early vs. late) × 2 (Brain Hemisphere: left vs. right) rmANOVA model. It revealed a significant interaction of Selected Deck Type - by - Task Stage - by - Brain Hemisphere ($F_{(1,24)}$ = 6.27, p = 0.020, η^2 = 0.207). The 2 (Selected Deck Types: good vs. bad) × 2 (Task Stages: early vs. late) interaction in the rmANOVA for the asymmetry index was also significant ($F_{(1,24)}$ = 6.27, p = 0.02, η^2 = 0.207). Simple effect analysis for asymmetry index reveled Task Stage differences that approach significance in the case of bad choices ($F_{(1,24)}$ = 3.03, p = 0.095, *Cohen's d* = 0.710) (Fig.6). This suggests that for disadvantageous decks (decks A and B), the activation in late stages showed a trend of right lateralization compared to early stages.

We then examined separately the left and right hemispheres of the mPFC. For the left mPFC, a 2 (Selected Deck Types: good vs. bad) × 2 (Task Stages: early vs. late) rmANOVA was estimated. It revealed no significant interaction (F(1,24) = 1.71, p = 0.203, η2 = 0.067) between Selected Deck Type and Task Stage. However, for the right mPFC, the same model demonstrated a significant interaction (F(1,24) = 5.26, p = 0.031, η2 = 0.180) between Selected Deck Type and Task Stage. A simple effect analysis showed a statistically significant difference between good and bad choices in the early stages of the IGT (F(1,24) = 7.54, p = 0.011, Cohen's d = 1.121). This suggests that in the early stages, the activity in the right mPFC was higher for good decisions than for bad decisions (Fig.5B). As such, the activation patterns of the left and right mPFC were different; the mPFC showed a tendency toward lateralized functional specificity that is a function of the IGT stage, as it shifts from early to late (or from under

ambiguity decision making condition to under risk decision making condition).

Lastly, Pearson correlations between bilateral averaged mPFC activations and IGT scores in the five blocks were calculated. Results revealed significant correlations between mPFC activation and IGT score in IGT2 ($r = 0.364$, $p = 0.037$), IGT3 ($r = 0.409$, $p = 0.021$) and IGT4 ($r = 0.456$, $p = 0.011$). See Fig.7B, Fig.7C and Fig.7D. mPFC activation was not significantly correlated with IGT1 scores ($r = -0.009$, $p = 0.483$) and IGT5 scores ($r = 0.090$, $p = 0.335$). See Fig.7A and Fig.7E.

4. Discussion

This study sought to examine important nuances of the mPFC's involvement in decision making under ambiguity and risk conditions. To our knowledge, this is the first study investigating the time course of mPFC activity, including hemispheric mPFC asymmetry in decision making under ambiguity and risk. It is also the first study analyzing fNIRS data using the FIR model. The current study confirms the primary hypothesis that the right mPFC likely plays a bigger role compared to the left mPFC in triggering "negative" somatic states that signal the avoidance of disadvantageous decisions. It also revealed hemisphere-specific temporal dynamic changes of mPFC activation in the course of decision-making under ambiguity and risk. We specifically found that (1) both left and right mPFC regions were activated during decision making; and that (2) the left and right mPFC can have different patterns of involvement in decision making, which may differ between advantageous and disadvantageous choices, and between decisions under ambiguity and under risk conditions. The present research therefore contributes to a deeper understanding of the role of the mPFC in decision making, re-affirms somatic marker hypothesis assumptions, and points to possible hemisphere-specific temporal

dynamic changes in mPFC activity during the IGT.

Consistent with previous studies [35,36], the current study reveals differences in the neural processing of decision making under ambiguity (the early stages of IGT) and decision making under risk (the late stages of IGT). Our results suggest that in the early stages of the IGT, the activity in the right mPFC is significantly higher for good decisions than for bad decisions, while in the late stages, the right mPFC activity is similar for bad and good decisions. However, such changes were not observed in the left mPFC, the activation of which did not differ between decision types (good/bad) and IGT stages (early/late). This is consistent with classic SMH studies that showed that somatic markers are triggered before good and bad decks, and are less discriminatory in early stages of the IGT [13, 17]. Here, we extend this view from SCR to mPFC activation.

Our findings specifically show that the two hemispheres of the mPFC are differently functionally involved in the process of decision making, as captured with the IGT. The demonstrated differences in hemodynamic changes of the left and right mPFC in the time course add new insights to the existing body of knowledge regarding the role of the mPFC in decision-making. The lateralization of signaling bad decisions to the right mPFC supports the original proposal of the SMH [14], and it is also consistent with some studies that found that IGT scores relate to activity in the right ventral prefrontal lobe, right insular and right caudate nucleus [11,37]. Note that right frontal lobes have also been linked to decision making in other decision-making under risk paradigms. For instance, the right PFC, as opposed to the left PFC, plays a key role in suppressing impulsions to make riskier choices in the balloon analog risk task (BART) and in gambling tasks [38-40]. Our results are aligned with such studies and

ultimately support the notion that as decision transition from ambiguity to risk conditions, at least as reflected in the IGT, the right hemisphere becomes more dominant.

Several limitations of this study need to be noted. First, the sample included mostly female participants. Nevertheless, males can exhibit stronger right hemisphere activation than females do [41,42]. In addition, damage to the right frontal region, rather than the left one, would interfere with IGT performance of males but not females [43]. Analysis of gender effects on PFC activity in decision-making was not performed in the present study given the small proportion of males we had. Hence, caution should be exercised regarding generalizing the results to male dominant samples; and future research should closely examine potential gender differences in mPFC activity lateralization. Second, the fNIRS technique is not sensitive to hemodynamic changes in deep brain regions. Future research can integrate fNIRS technology with other imaging technologies, such as fMRI, building on the strengths of each technology and creating synergy [44]. Last, we assumed that the division between early and late stages of the IGT parallels the division between decision making under ambiguity and under risk conditions and that this division is similar for all participants. Future research should consider capturing the level of ambiguity and/or risk understanding during the IGT stages and also consider examining person-specific cutoffs between the ambiguity and risk phases.

5. Conclusions

The results demonstrate that the left and right mPFC have different patterns of involvement in decision making under ambiguity and under risk conditions. These findings advance our understanding of the dynamic neural mechanisms involved in complex decision

making as situations transition from ambiguous risk profiles into states of understandable risk rules.

Acknowledgements

References

[1] Hastie, R. Problems for Judgment and Decision Making. Annual Review of Psychology. 52 (1) (2001) 653.

[2] Bos, R. V. D., Homberg, J., & Visser, L. D. A critical review of sex differences in decision-making tasks: Focus on the Iowa Gambling Task. Behavioural Brain Research. 238 (1) (2013) 95-108.

[3] Fox, C. R., & Poldrack, R. A. Prospect Theory and the Brain - Neuroeconomics - Chapter 11. Neuroeconomics. (2009) 145–173.

[4] He, Q., Xue, G., Chen, C., Lu, Z., Dong, Q., Lei, X., . . . Chen, C. Serotonin Transporter Gene-Linked Polymorphic Region (5-HTTLPR) Influences Decision Making under Ambiguity and Risk in a Large Chinese Sample. Neuropharmacology. 59 (6) (2010) 518-526.

[5] He, Q., Xue, G., Chen, C., Lu, Z. L., Chen, C., Lei, X., . . . Moyzis, R. K. COMT Val158Met polymorphism interacts with stressful life events and parental warmth to influence decision making. Scientific Reports. 2 (4) (2012) 677.

[6] O. Feldmanhall, P. Glimcher, A.L. Baker, E.A. Phelps, Emotion and decision-making under uncertainty: Physiological arousal predicts increased gambling during ambiguity but not risk, J Exp Psychol Gen 145(10) (2016) 1255-1262.

[7] Bechara, A., Damasio, A. R., Damasio, H., & Anderson, S. W. Insensitivity to future consequences following damage to human prefrontal cortex. Cognition. 50 (1–3) (1994) 7-15.

[8] A.L. Krain, A.M. Wilson, R. Arbuckle, F.X. Castellanos, M.P. Milham, Distinct neural mechanisms of risk and ambiguity: a meta-analysis of decision-making, Neuroimage 32(1) (2006) 477-484.

[9] M.E. Toplak, G.B. Sorge, A. Benoit, R.F. West, K.E. Stanovich, Decision-making and cognitive abilities: A review of associations between Iowa Gambling Task performance, executive functions, and intelligence, Clinical Psychology Review 30(5) (2010) 562-581.

[10] Brand, M., Recknor, E., Grabenhorst, F., & Bechara, A. Decisions under ambiguity and decisions under risk: correlations with executive functions and comparisons of two different gambling tasks with implicit and explicit rules. Journal of clinical and experimental neuropsychology. 29 (1) (2007) 86.

[11] Ernst, M., Bolla, K., Mouratidis, M., Contoreggi, C., Matochik, J. A., Kurian, V., . . . London, E. D. Decision-making in a risk-taking task: a PET study. Neuropsychopharmacology : official publication of the American College of Neuropsychopharmacology. 26(5) (2002) 682.

[12] Li, X., Lu, Z. L., D'Argembeau, A., Ng, M., & Bechara, A. The Iowa Gambling Task in fMRI images. Human Brain Mapping. 31 (3) (2010) 410.

[13] Bechara, A., Damasio, H., Tranel, D., & Damasio, A. R. Deciding advantageously before knowing the advantageous strategy. Science. 275 (5304) (1997) 1293-1295.

[14] Damasio, A. R. Descartes' error: Emotion, rationality and the human brain. (1994)

[15] Damasio, A. R. The somatic marker hypothesis and the possible functions of the prefrontal cortex. Philosophical Transactions of the Royal Society of London. 351 (1346) (1996) 1413-1420.

[16] Bechara, A. The somatic marker hypothesis: A neural theory of economic decision. Games and Economic Behavior. 52 (2) (2005) 336-372.

[17] Bechara, A., Tranel, D., Damasio, H., & Damasio, A. R. Failure to respond autonomically to anticipated future outcomes following damage to prefrontal cortex. Cerebral Cortex. 6 (2) (1996) 215-225.

[18] Ferrari, M., & Quaresima, V. A brief review on the history of human functional near-infrared spectroscopy (fNIRS) development and fields of application. Neuroimage. 63 (2) (2012) 921-935.

[19] Boas, D. A., Elwell, C. E., Ferrari, M., & Taga, G. Twenty years of functional near-infrared spectroscopy: introduction for the special issue. Neuroimage. 85 (1, 1) (2014) 1-5.

[20] Bembich, S., Clarici, A., Vecchiet, C., Baldassi, G., Cont, G., & Demarini, S. Differences in time course activation of dorsolateral prefrontal cortex associated with low or high risk choices in a gambling task. Frontiers in Human Neuroscience. 8 (2014) 464.

[21] Lópezramos, J. C., Guerranarbona, R., & Delgadogarcía, J. M. Different forms of decision-making involve changes in the synaptic strength of the thalamic, hippocampal, and amygdalar afferents to the medial prefrontal cortex. Frontiers in Behavioral Neuroscience. 9 (2015) 7.

[22] Tartaglione, A., Inglese, M. L., Bandini, F., Spadavecchia, L., Hamsher, K., & Favale, E. HEMISPHERE ASYMMETRY IN DECISION MAKING ABILITIES: AN EXPERIMENTAL STUDY IN UNILATERAL BRAIN DAMAGE. Brain. 114 (pt 3) (3) (1991) 1441-1456.

[23] Vendetti, M. S., Johnson, E. L., Lemos, C. J., & Bunge, S. A. Hemispheric Differences in Relational Reasoning: Novel Insights Based on an Old Technique. Frontiers in Human Neuroscience. 9 (2015) 55.

[24] He, Q., Chen, M., Chen, C., Xue, G., Feng, T., & Bechara, A. Anodal Stimulation of the Left DLPFC Increases IGT Scores and Decreases Delay Discounting Rate in Healthy Males. Frontiers in Psychology. 7 (2016) 1-4.

[25] He, Q., Xiao, L., Xue, G., Wong, S., Ames, S. L., Xie, B., & Bechara, A. Altered dynamics between neural systems sub-serving decisions for unhealthy food. Frontiers in Neuroscience. 8 (2014) 350.

[26] Bechara, A., Damasio, H., Damasio, A. R., & Lee, G. P. Different contributions of the human amygdala and ventromedial prefrontal cortex to decision-making. Journal of Neuroscience the Official Journal of the Society for Neuroscience. 19 (13) (1999) 5473-5481.

[27] Delpy, D. T., Cope, M., Zee, P. v. d., Arridge, S., Wray, S., & Wyatt, J. Estimation of optical pathlength through tissue from direct time of flight measurement. Physics in medicine and biology. 33(12) (1988) 1433-1442.

[28] Koritzky, G., He, Q., Xue, G., Wong, S., Xiao, L., & Bechara, A. Processing of time within the prefrontal cortex: recent time engages posterior areas whereas distant time engages anterior areas. Neuroimage. 72 (10) (2013) 280-286.

[29] Hoshi, Y. Functional near-infrared spectroscopy: Current status and future prospects. Journal of Biomedical Optics. 12 (6) (2007) 062106.

[30] Jiang, J., Chen, C., Dai, B., Shi, G., Ding, G., Liu, L., & Lu, C. Leader emergence through interpersonal neural synchronization. Proceedings of the National Academy of Sciences of the United States of America. 112 (14) (2015) 4274-4279.

[31] Henson, R., Rugg, M. D., & Friston, K. J. The choice of basis functions in event-related fMRI. Neuroimage. 13 (6) (2001) 149-149.

[32] Poldrack, R. A., Mumford, J. A., & Nichols, T. E. Handbook of functional MRI data analysis. Cambridge University Press. (2011)

[33] Miezin, F. M., Maccotta, L., Ollinger, J. M., Petersen, S. E., & Buckner, R. L. Characterizing the Hemodynamic Response: Effects of Presentation Rate, Sampling Procedure, and the Possibility of Ordering Brain Activity Based on Relative Timing. Neuroimage. 11 (1) (2000) 735-759.

[34] Vigneau, M., Jobard, G., Mazoyer, B., & Tzourio-Mazoyer, N. Word and non-word reading: what role for the Visual Word Form Area? Neuroimage. 27 (3) (2005) 694.

[35] Homberg, J., Van-Den-Bos, R., Den-Heijer, E., R, & Cuppen, E. Serotonin transporter dosage modulates long-term decision-making in rat and human. Neuropharmacology. 55 (1) (2008) 80-84.

[36] Van, d. B. R., Homberg, J., Gijsbers, E., Den, H. E., & Cuppen, E. The effect of COMT Val158 Met genotype on decision-making and preliminary findings on its interaction with the 5-HTTLPR in healthy females. Neuropharmacology. 56 (2) (2009) 493.

[37] Bolla, K. I., Eldreth, D. A., London, E. D., Kiehl, K. A., Mouratidis, M., Contoreggi, C., . . . Kimes, A. S. Orbitofrontal cortex dysfunction in abstinent cocaine abusers performing a decision-making task. Neuroimage. 19 (3) (2003) 1085-1094.

[38] Knoch, D., Gianotti, L. R., Pascual-Leone, A., Treyer, V., Regard, M., Hohmann, M., & Brugger, P. Disruption of right prefrontal cortex by low-frequency repetitive transcranial magnetic stimulation induces risk-taking behavior. Journal of Neuroscience. 26 (24) (2006) 6469-6472.

[39] Fecteau, S., Knoch, D., Fregni, F., Sultani, N., Boggio, P., & Pascualleone, A. Diminishing risk-taking behavior by modulating activity in the prefrontal cortex: A direct current stimulation study. Journal of Neuroscience the Official Journal of the Society for Neuroscience. 27 (46) (2007) 12500.

[40] Fecteau, S., Pascualleone, A., Zald, D. H., Liguori, P., Théoret, H., Boggio, P. S., & Fregni, F. Activation of prefrontal cortex by transcranial direct current stimulation reduces appetite for risk during ambiguous decision making. Journal of Neuroscience the Official Journal of the Society for Neuroscience. 27 (23) (2007) 6212.

[41] Bolla, K. I., Eldreth, D. A., Matochik, J. A., & Cadet, J. L. Sex-related Differences in a Gambling Task and Its Neurological Correlates. Cerebral Cortex. 14 (11) (2004) 1226-1232.

[42] Wager, T. D., Phan, K. L., Liberzon, I., & Taylor, S. F. Valence, gender, and lateralization of functional brain anatomy in emotion: a meta-analysis of findings from neuroimaging. Neuroimage. 19 (3) (2003) 513-531.

[43] Tranel, D., Damasio, H., Denburg, N. L., & Bechara, A. Does gender play a role in functional asymmetry of ventromedial prefrontal cortex? Digest of the World Core Medical Journals. 128 (Pt 12) (2005) 2872-2881.

[44] Liu, N., Cui, X., Bryant, D. M., Glover, G. H., & Reiss, A. L.. Inferring deep-brain activity from cortical activity using functional near-infrared spectroscopy. Biomedical Optics Express. 6 (3) (2015) 1074-1089.

[45] Xia, M., Wang, J., & Yong, H. BrainNet Viewer: A Network Visualization Tool for Human Brain Connectomics. PLoS ONE. 8(7) (2013) e68910.

Tables

Table 1: Probabilistic cortical channels localization of channels within ROIs (the left and right mPFC regions) in MNI space

Channel	Anatomical label	MNI coordinates estimation (mm)			
		x	y	z	SD
25	R middle frontal gyrus	33	59	25	7.3
28	L middle frontal gyrus	-23	62	27	7.0
32	R middle frontal gyrus	43	59	14	5.4
33	R middle frontal gyrus	26	69	16	5.7
35	L middle frontal gyrus	-16	71	17	5.4
36	L middle frontal gyrus	-36	60	17	6.0
40	R middle frontal gyrus	39	64	5	5.1
41	R middle frontal gyrus	20	73	7	5.0
42	L middle frontal gyrus	-9	73	9	7.7
43	L middle frontal gyrus	-27	68	9	5.7

R, right; L, left.

Legends for Figures

Figure 1: An illustration of the IGT. A) Participants were instructed to select one card from four decks. B) After each selection, they are shown how much money they win, and C) sometimes, they are also shown how much money they lose. D) The behavioral results showed that participants learned to make better choices as the task progressed (error bars represent standard deviations).

Figure 2: Channel arrangement and channel contained in the region of interest in present study. A) Schematic diagram of the channel file in the experiment. Red circles represent the transmitting fiber-optic probes, and blue circles represent the receiving fiber-optic probes. The parts between two adjacent transmitting and receiving fiber-optic probes represent the channels. There was a total of 52 channels; B) co-registration of fNIRS channel locations on a human brain template with frontal view. Numbers represent channel numbers and locations, blue circles represent the interested channel; C) The selected left and right medial prefrontal cortex ROIs. The left medial prefrontal cortex includes channel numbers 28, 35, 36, 42, and 43, and the right medial prefrontal cortex includes channel numbers 25, 32, 33, 40, and 41. The mapping is presented in frontal view with BrainNet Viewer [45].

Figure 3: Averaged performance on IGT for all subjects. The shaded area indicates 95% Confidence Interval.
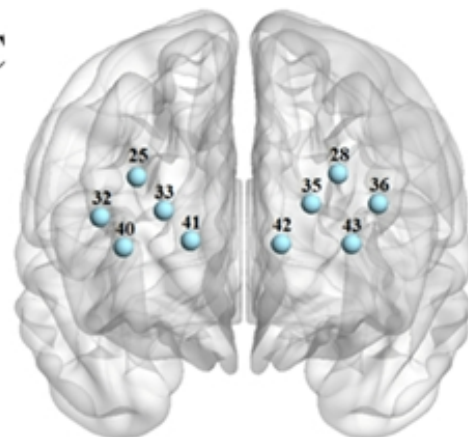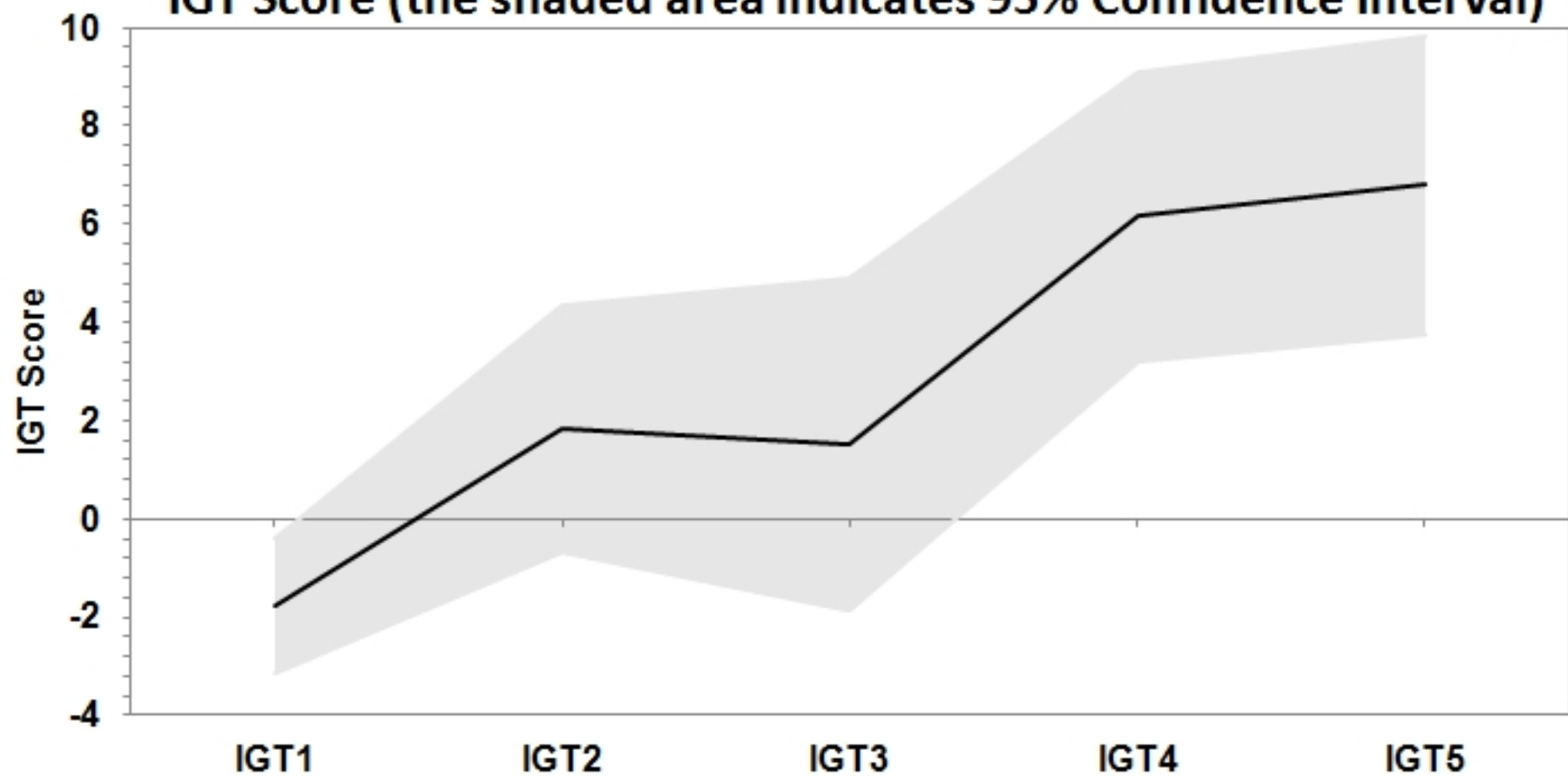
Figure 4: Results of activity check. Activation map of HbO signals using maximum value of

ten channels covering the left and right mPFC for all participants (N = 25) in conditions of (a) early-good, (b) early-bad, (c) late-good, and (d) late-bad.

Figure 5: The results of time course map. A) Average time course map of brain activity of left mPFC and right mPFC in all participants (n = 25), in four conditions including early-good (red), early-bad (yellow), late-good (green) and late-bad (blue); B) Statistical differences between good and bad deck selections and between early and late stages in terms of HbO in the left and right mPFC regions (*$p < 0.05$).

Figure 6: Statistical results of asymmetry index comparison between good and bad deck selections and between early and late stages ([a]$p < 0.1$).

Figure 7: Brain-behavior correction of mPFC in five blocks. There was a significant positive correlation between Brain activity (HbO) and IGT score in IGT2 (B), IGT3 (C) and IGT4 (D)., while it had not reached a significant level in IGT1 (A) and IGT5 (E).

Figure panels:
- A: 当前金额 / 借款金额; 请选择; A' B' C' D'
- B: 当前金额 / 借款金额; 赢了 ＄60！; A' B' C' D'
- C: 当前金额 / 借款金额; 输了 ＄150！; A' B' C' D'
- D: IGT score vs Task stage (IGT1, IGT2, IGT3, IGT4, IGT5)
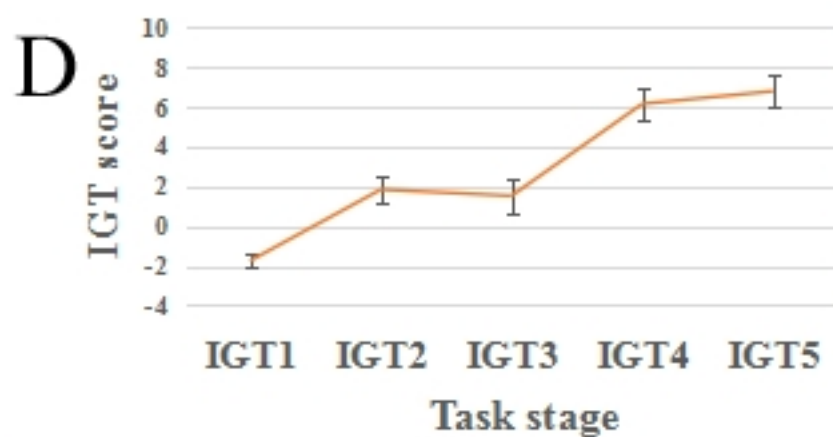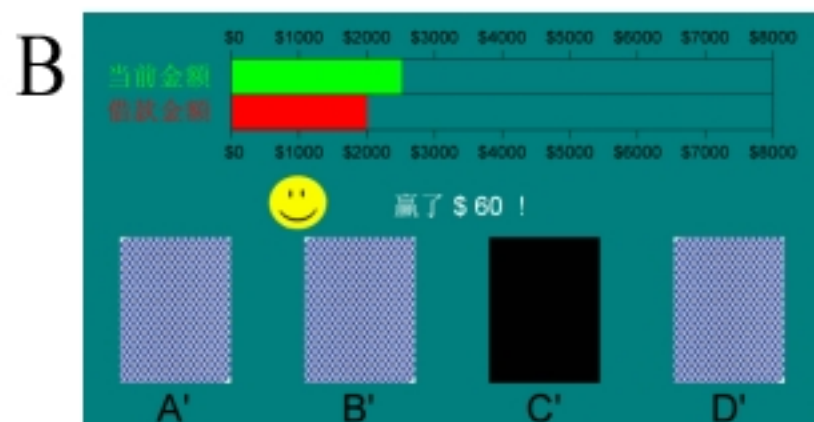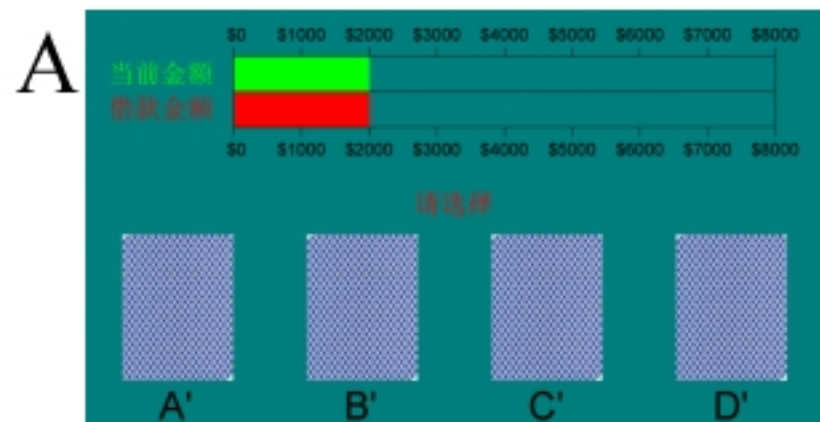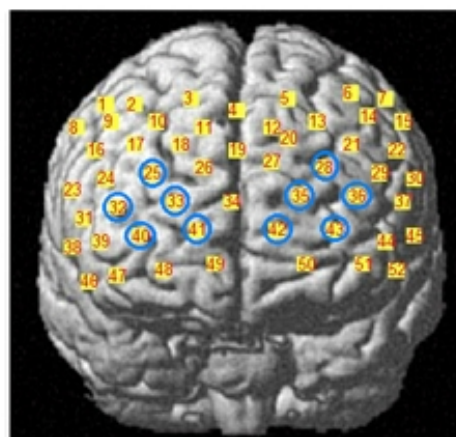
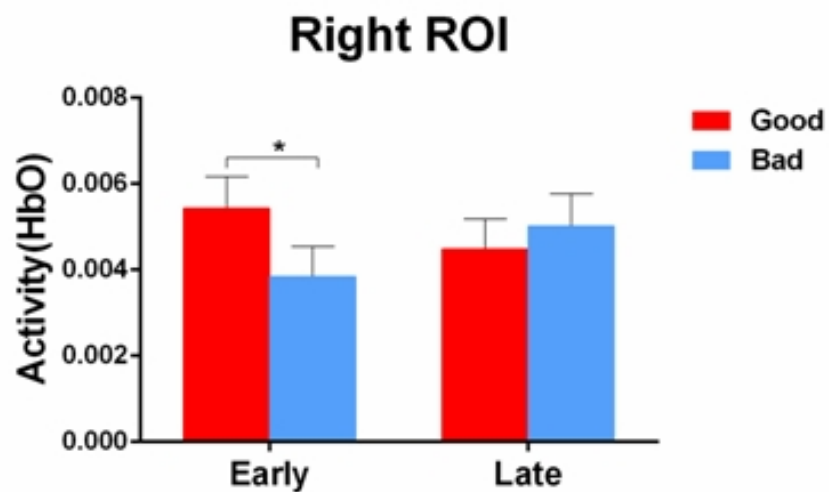**IGT Score (the shaded area indicates 95% Confidence Interval)**

early

late

good

bad

(a)

(c)

(b)

(d)
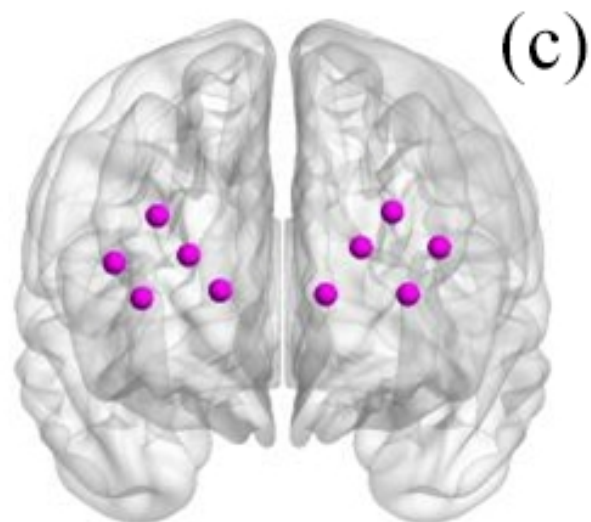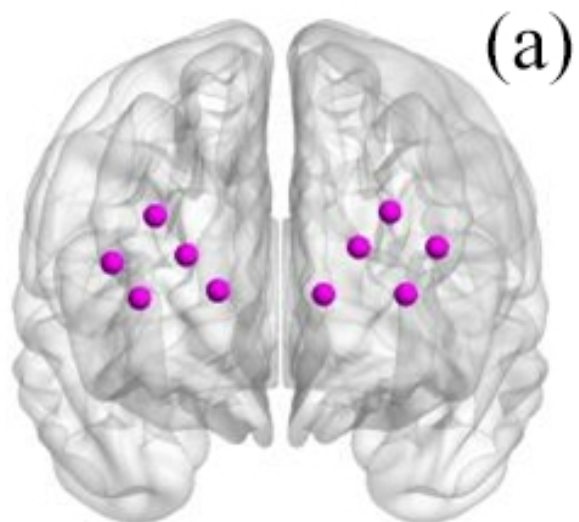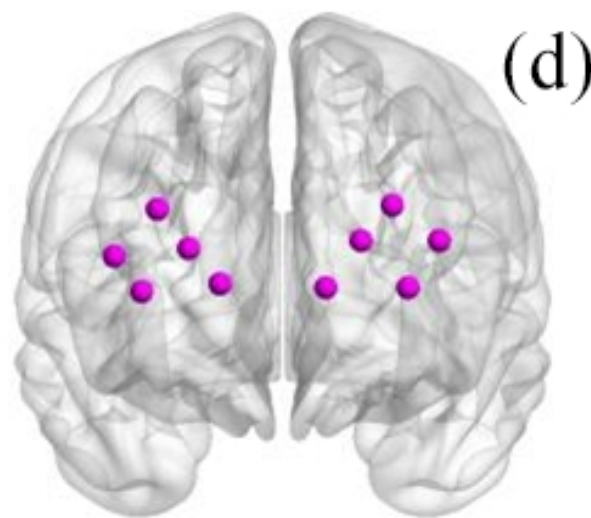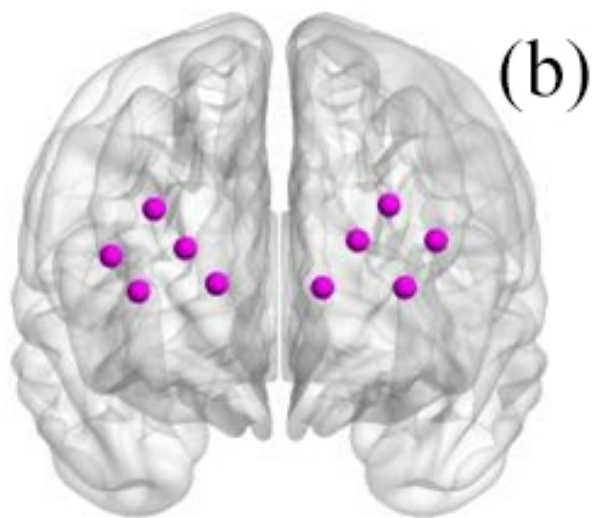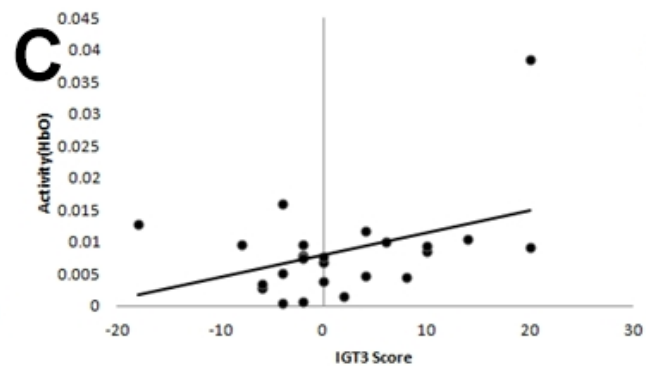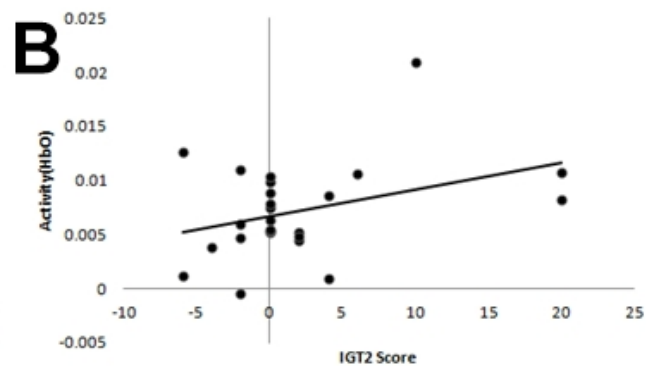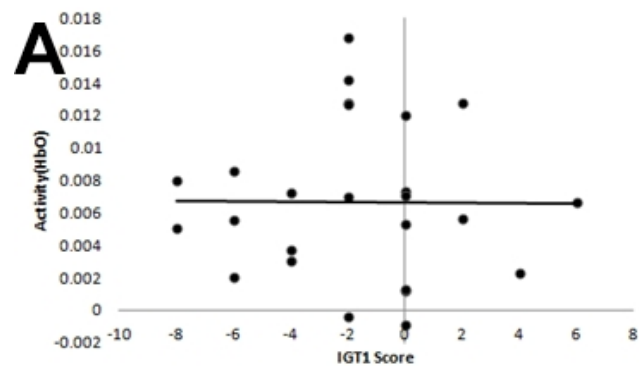
p<0.05
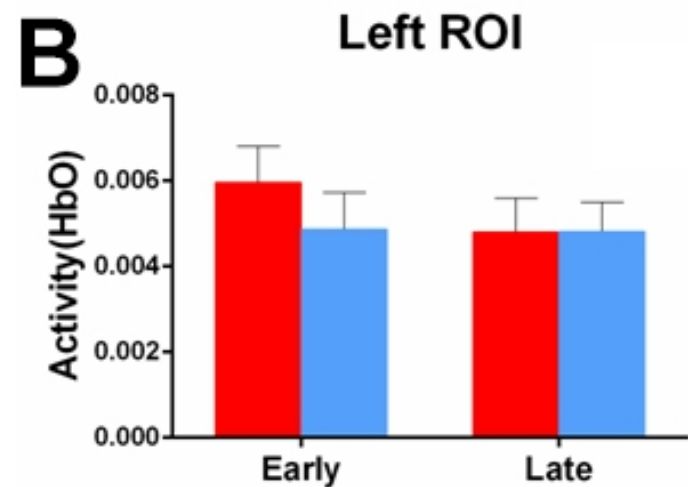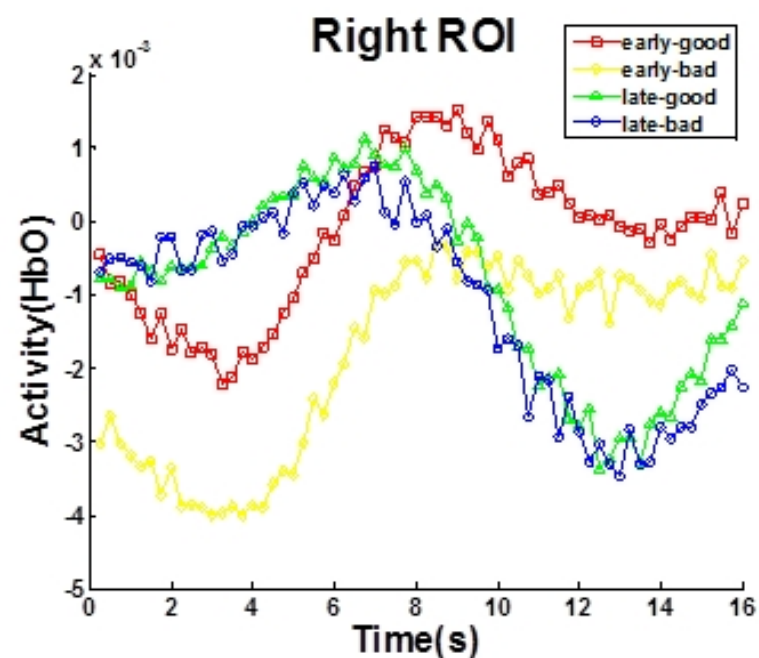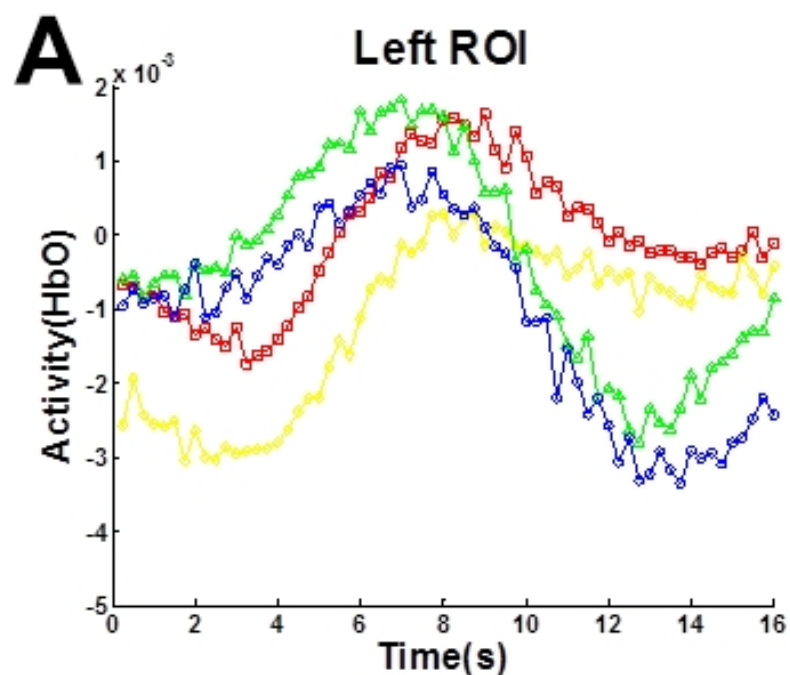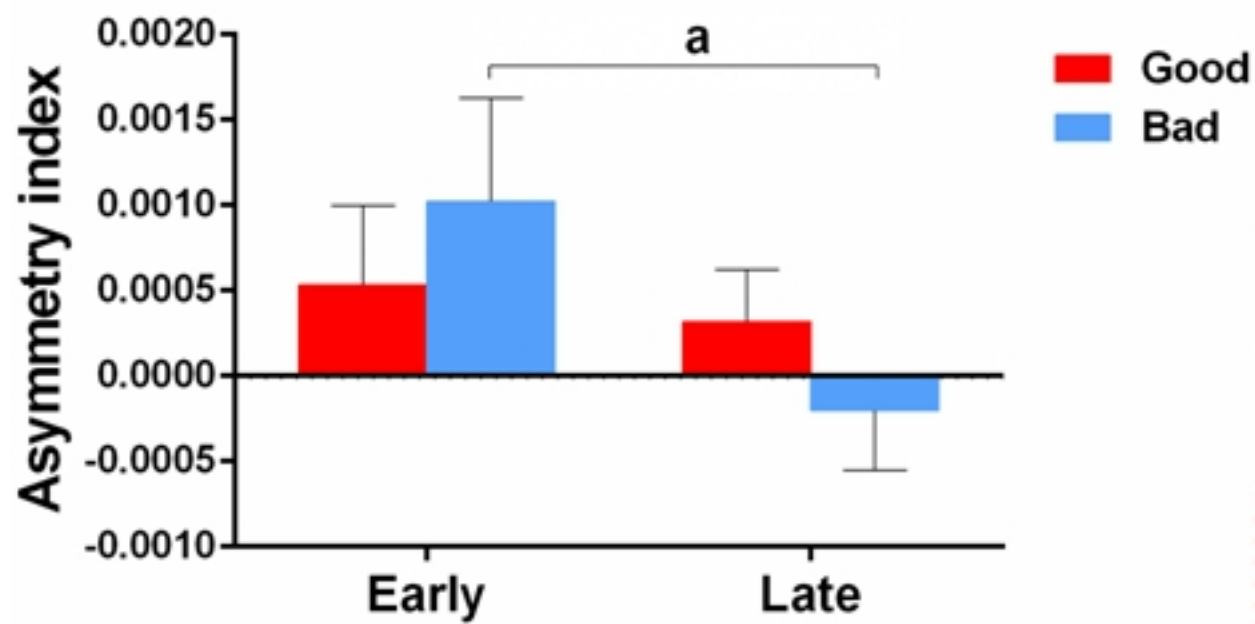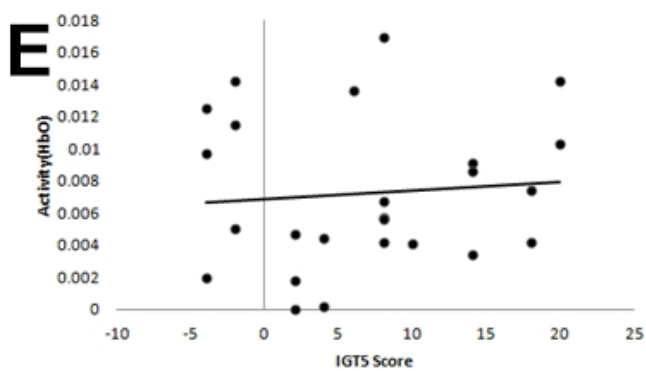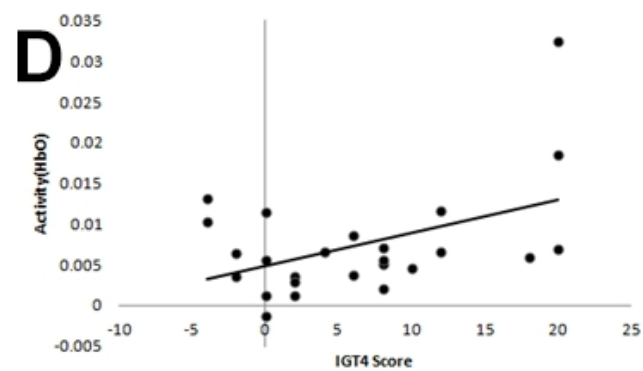
In the main text of the manuscript, we describe an analysis comparing activations in decisions

under ambiguity vs. risk conditions, using transition points implied by the pattern of IGT

scores in the data. Here, we present the same analysis, but when using a commonly employed

crude-division of the ITG into under-ambiguity (first 40 trials) and under risk (last 60 trials)

stages. As can be seen, the results are largely consistent with analysis we present in the main

text. This increases the validity of our assertions and imply that the results may not depend on

the specifics of the employed cutoff, as long as this cutoff is within the middle set of IGT

blocks.

Results of Supplementary Analysis

Behavioral data

The Iowa Gambling Task scores were first analyzed by five blocks of 20 trials following

the procedure used in previous studies [6]. One-factor ANOVA with repeated measures with

the IGT scores of five different blocks as a within-subject factor suggested that there was a

significant learning effects; over time as IGT progressed, participants learned to choose more

often good decks over bad ones ($F_{(4,96)} = 10.493$, $p < 0.001$, $\eta^2 = 0.304$). Post hoc test showed

that both blocks 4 and 5 had significantly higher IGT scores, compared to the former three

blocks (i.e., blocks 1, 2 and 3; least significant difference test [LSD], $p < 0.05$). In addition,

block 2 showed a higher IGT score, compared to block 1 (post hoc: $p < 0.05$), and there was

also somewhat higher (approaching significance) IGT score in block 3, compared to block 1

(post hoc: $p = 0.057$). Furthermore, a paired sample t test comparing early stage (the first 40

trials, i.e., block1 + block2) and late stage (the last 60 trials, i.e., block3 + block4 + block5)

showed that there was a significant difference between the early and the late stages in IGT scores (M_{late}=4.83, M_{early}=0.04, $t_{(24)}$= 4.77, p < 0.001, *Cohen's d* = 1.947), suggesting that participants learned to choose more often from good decks in the late stage relative to the early stage. Given that the subjects were cognitively healthy, the improvement in IGT scores can be reasonably attributed to learning processes, which include inferences regarding the rules of the loss and gain function in the IGT task.

fNIRS data

Both left and right mPFC regions were activated during decision making

We commenced analysis with a channel-wise activity check. Results suggested that almost every channel within the left and right mPFC was significantly active during the four different conditions of the task, except for channel 43 in early good choices, channels 33, 41, and 35 in late good choices, channels 25, and 32 in early bad choices, and channel 28 in late bad decisions (Fig.S1). That is, most of these channels showed a significant hemodynamic response to the stimulus in each decision making condition.

The left and right mPFC have different levels of involvement in decision making under ambiguity and under risk conditions

To reduce the number of comparisons, we averaged the hemodynamic signals from each channel within each ROI. Fig.S2A plots the average time course map of left and right mPFC over all participants in different conditions. The progression pattern highlights the centrality of the mPFC in decision making. It also illuminates possible differences between early and late decision stages, as well as between good and bad choices. The differences between the activity progression lines, each representing a different decision stage (early/late) and choice type

(good/bad), hints at possible differential involvement of the mPFC in different decision stages and choices.

Next, we tested whether there are left and right mPFC activation differences between IGT stages and decision types. To do so, we performed a 2 (Selected Deck Types: good vs. bad) × 2 (Task Stages: early vs. late) × 2 (Brain Hemisphere: left vs. right) repeated-measures ANOVA. It revealed a significant Selected Deck Type - by - Task Stage - by - Brain Hemisphere interaction ($F_{(1,24)}$ = 6.32, p = 0.019, η^2 = 0.209). Similarly, a 2 (Selected Deck Types: good vs. bad) × 2 (Task Stages: early vs. late) repeated-measures ANOVA for the asymmetry index revealed a significant interaction between Selected Deck Type and Task Stage ($F_{(1,24)}$ = 6.32, p = 0.19, η^2 = 0.209). A follow-up simple effect analysis for the asymmetry index reveled that Task Stage differences were somewhat pronounced in bad Deck Type choices (differences approached significance: $F_{(1,24)}$ = 3.68, p = 0.067, *Cohen's d* = 0.783). See also Fig.S3. This suggests that for bad decks (decks A and B), the activation in late stage showed a trend of right lateralization compared to that in the early stage, which approached significance.

We also tested whether there is a left and right mPFC activation difference between different IGT conditions via two-way interactions. For the left mPFC, a 2 (Selected Deck Types: good vs. bad) × 2 (Task Stages: early vs. late) repeated-measures analysis of variance (ANOVA) was conducted. It revealed a significant interaction between Selected Deck Type and Task Stage ($F_{(1,24)}$ = 10.11, p = 0.004, η^2 = 0.296). The analysis of simple effects reveled that only Selected Deck Type differences in the early Task Stage had an effect that approached significance: $F_{(1,24)}$ = 3.76, p = 0.064, *Cohen's d* = 0.792. See also Fig.S2B. This suggested that in early stage, choosing good decks activated the left mPFC slightly more than choosing bad

decks.

We found a significant interaction for the right mPFC, between Selected Deck Type and Task Stage ($F_{(1,24)}$ = 14.61, p = 0.001, η^2= 0.378). The simple effect analysis showed that there were statistically significant differences between good and bad choices in the early stage and late stage [early: $F_{(1,24)}$ = 8.83, p = 0.007, *Cohen's d* = 1.213; and late: $F_{(1,24)}$ = 5.09, p = 0.033, *Cohen's d* = 0.921]. Moreover, there was a significant difference between early and late stages in bad choice ($F_{(1,24)}$ = 5.07, p = 0.034, *Cohen's d* = 0.919), but not in good choice in HbO activity (Fig.S2B). That is, the activations of left and right mPFC differed, implying that the mPFC can present lateralized functional specificity in IGT tasks as the task transitions from early to late stages, which may be conceived as paralleling the transition from decision-making under ambiguity to under risk.

To enrich the abovementioned findings, two extra parameters, i.e., peak time point and regression coefficient, were calculated to represent the latency (the difference between the time point of stimulus presentation and the point where the HRF signal reaches maximum value) and rising (the regression coefficient for the slope between activity value of stimulus presentation and HRF peak) of the HbO concentration. Similar ANOVA models to these used in the abovementioned analyses were applied to these two parameters.

For the latency of HRF in the left mPFC, only main effect of Stage ($F_{(1,24)}$ = 3.63, p = 0.069, η^2 = 0.131) was approaching significance. Late choices showed faster HRF peaking than early choices did, especially in good choices ($t_{(24)}$ = 3.31, p = 0.003, *Cohen's d* = 1.351). For the right mPFC, only the main effect of Stage was significant ($F_{(1,24)}$ = 8.40, p = 0.008, η^2= 0.259). Late trials showed faster HRF than early trials, in both good choices ($t_{(24)}$ = 2.46, p =

0.021, *Cohen's d* = 1.006) and bad choices ($t_{(24)}$ = 2.57, p = 0.017, *Cohen's d* = 1.049). Together, these results imply that late good choices involved faster activation peaking in the mPFC, bilaterally.

For HbO rising in the left mPFC, only main effect of Stage was approaching significance ($F_{(1,19)}$ = 3.68, p = 0.070, η^2 = 0.162). The rising of HRF was steeper for late good trials than for early good trials ($t_{(22)}$ = 2.02, p = 0.056, *Cohen's d* = 0.862). In the right mPFC, the main effects of Type ($F_{(1,22)}$ = 5.56, p = 0.028, η^2 = 0.202) and Stage ($F_{(1,22)}$ = 12.72, p = 0.002, η^2 = 0.366) were significant. This suggests that late good trials are characterized by steeper HRF signal change compared to early good trials($t_{(24)}$ = 2.59, p = 0.016, *Cohen's d* = 1.059). The HRF signal change was also steeper in late good trials than in late bad trials ($t_{(22)}$ = 2.47, p = 0.022, *Cohen's d* = 1.053); early bad trials showed the least steep change in HbO ($t_{(22)}$ = 2.11, p = 0.046, *Cohen's d* = 0.901).

In addition, Pearson correlations were computed on brain activity of right ROI and IGT score in five blocks, separately. We found significant correlations between brain activation of right mPFC and IGT score in later stages (i.e., IGT3: r = 0.414, p = 0.020; IGT4: r = 0.425, p = 0.017). See Fig.S4C and Fig.S4D. Although there was also a positive trend in the association between brain and behavior in IGT1, IGT2 and IGT5, it had not reached a significant level (i.e., IGT1: r = 0.127, p = 0.273; IGT2: r = 0.309, p = 0.067; IGT5: r = 0.028, p = 0.448). See Fig.S4A, Fig.S4B and Fig.S4E.

Legends for Figures

Figure S1: Results of activity check. Activation map of HbO signals using maximum value of ten channels covering the left and right mPFC for all participants (n = 25) in conditions of (a) early-good, (b) early-bad, (c) late-good, and (d) late-bad.

Figure S2: The results of time course map. A) Average time course map of brain activity of left mPFC and right mPFC in all participants (n = 25), in four conditions including early-good (red), early-bad (yellow), late-good (green) and late-bad (blue); B) Statistical differences between good and bad deck selections and between early and late stages in terms of HbO in the left and right mPFC regions; C) Statistical differences between good and bad deck selections and between early and late stages in terms of regression coefficient related to the left and right mPFC regions; D) Statistical differences between good and bad deck selections and between early and late stages in terms of time point arriving to peak HbO value in the left and right mPFC regions ($^a p < 0.1$; $*p < 0.05$; $**p < 0.01$; ns, not significant).

Figure S3: Statistical results of asymmetry index comparison between good and bad deck selections and between early and late stages ($^a p < 0.1$; $*p < 0.05$; $**p < 0.01$; ns, not significant).

Figure S4: Brain-behavior correlation of right ROI in five blocks. There was a significant positive correlation between brain activity (HbO) and IGT score only in IGT3 (C) and IGT4 (D). Although there was also a positive trend in the relationship between brain and behavior in IGT1 (A), IGT2 (B) and IGT5 (E), it did not reach significance at least at $p<0.05$.
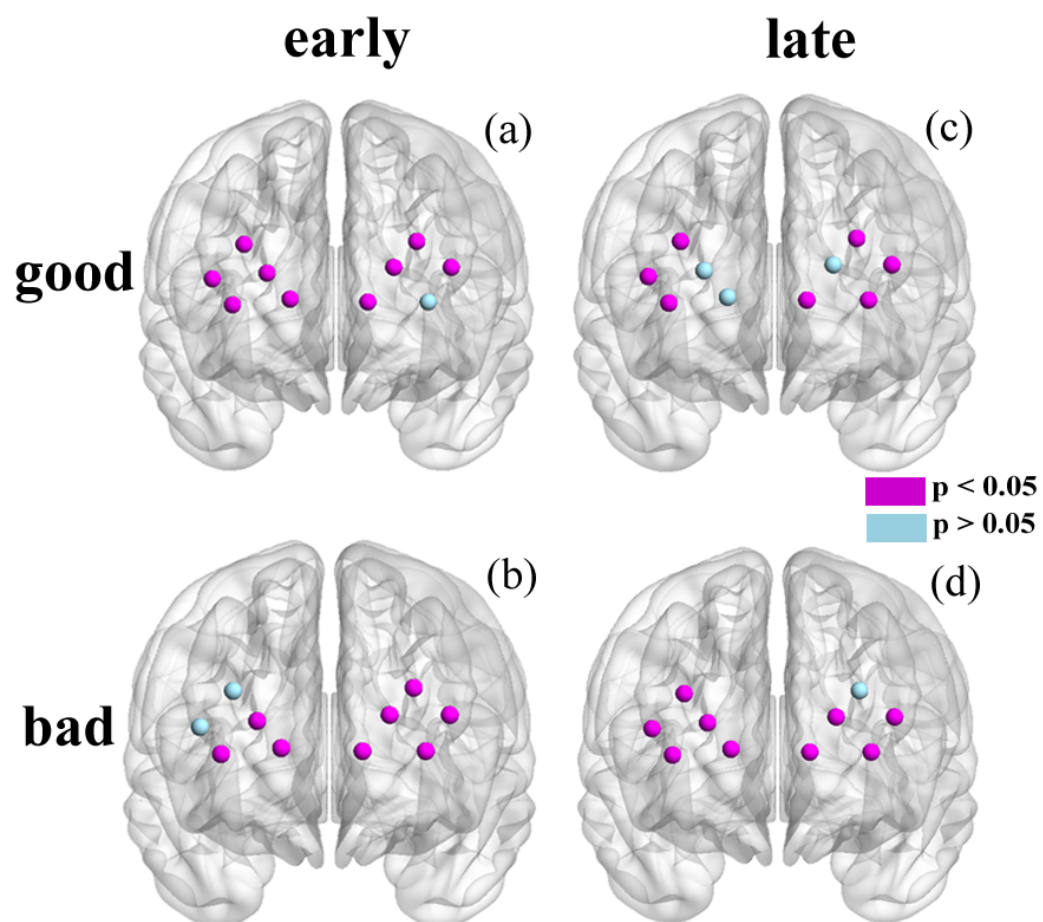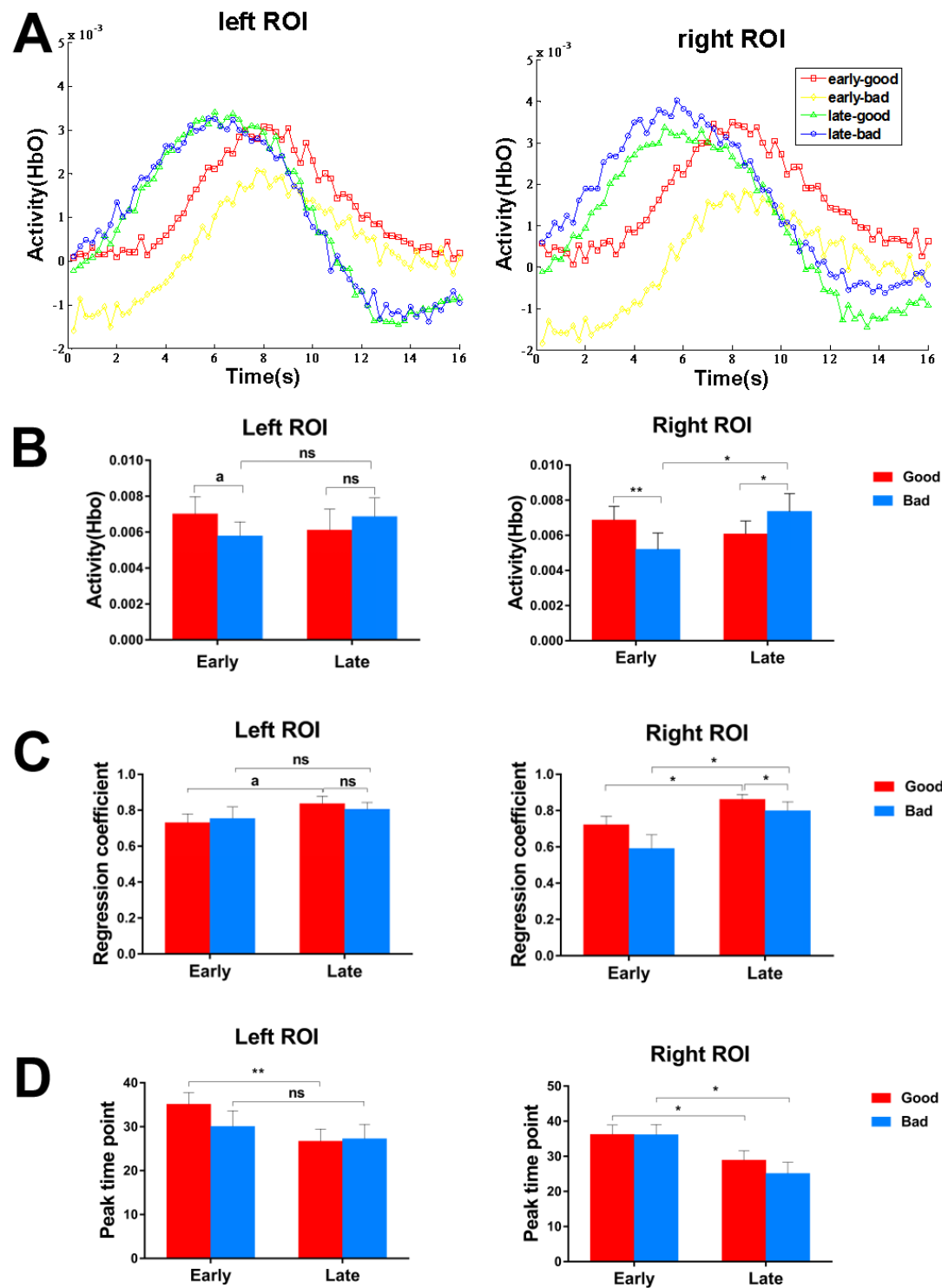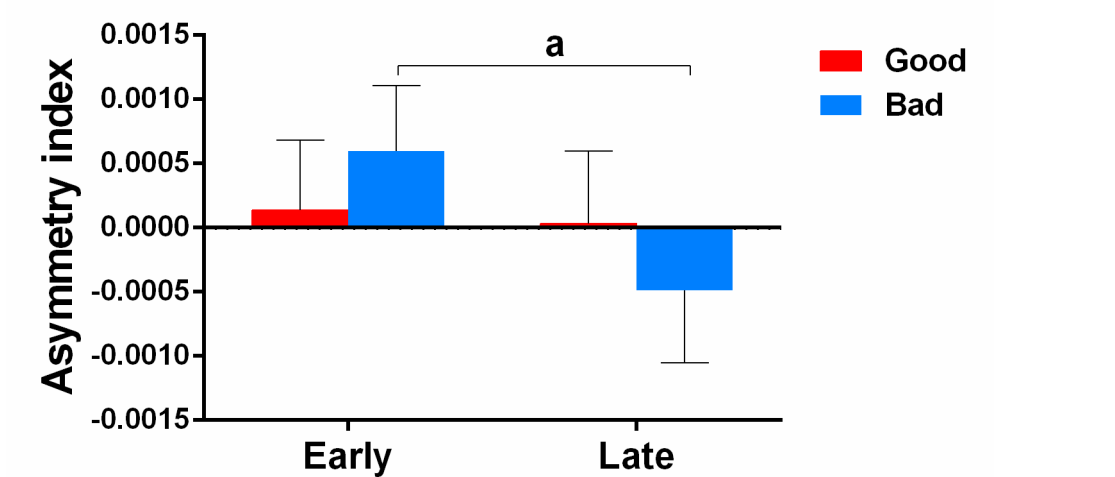
Figure S1

Figure S2

Figure S3

Figure S4